

MEASUREMENT OF LIGHT-CONE WAVE FUNCTIONS  
BY DIFFRACTIVE DISSOCIATION

DANIEL ASHERY

*School of Physics and Astronomy, Sackler Faculty of Exact Science, Tel Aviv University,  
Tel Aviv 69978, Israel*

Received 14 September 2003; Accepted 26 April 2004

Online 10 October 2004

Diffractive dissociation of particles can be used to study their light-cone wave functions. Results are presented for the pion from Fermilab experiment E791 and for the photon from HERA/ZEUS experiment at DESY.

PACS numbers: 13.60.-r

UDC 539.12

Keywords: hadronic structure, diffractive dissociation, light-cone wave functions

## 1. The pion light-cone wave function

### 1.1. Theoretical considerations

A very powerful description of the hadronic structure is obtained through the light-cone wave functions (LCWF). These functions are constructed from the QCD light-cone Hamiltonian:  $H_{LC}^{QCD} = P^+ P^- - P_{\perp}^2$  where  $P^{\pm} = P^0 \pm P^z$  with  $P$  the momentum operators [1]. The LCWF  $\psi_h$  for a hadron  $h$  with mass  $M_h$  satisfies the relation:  $H_{LC}^{QCD} |\psi_h\rangle = M_h^2 |\psi_h\rangle$ . Measurement of the LCWF can therefore test the interaction described by the Hamiltonian. The LCWF are expanded in terms of a complete basis of Fock states having increasing complexity [1]. For example, the negative pion has the Fock expansion

$$\begin{aligned}
 |\psi_{\pi^-}\rangle &= \sum_n \langle n | \pi^- \rangle |n\rangle \\
 &= \psi_{d\bar{u}/\pi}^{(\Lambda)}(u_i, \vec{k}_{\perp i}) |\bar{u}d\rangle + \psi_{d\bar{u}g/\pi}^{(\Lambda)}(u_i, \vec{k}_{\perp i}) |\bar{u}dg\rangle + \dots
 \end{aligned}
 \tag{1}$$

They have longitudinal light-cone momentum fractions

$$u_i = \frac{k_i^+}{p^+} = \frac{k_i^0 + k_i^z}{p^0 + p^z}, \quad \sum_{i=1}^n u_i = 1 \quad (2)$$

and relative transverse momenta

$$\vec{k}_{\perp i}, \quad \sum_{i=1}^n \vec{k}_{\perp i} = \vec{0}_{\perp}, \quad (3)$$

where the index  $i$  runs over the particles contained in the relevant Fock state. The first term in the expansion is referred to as the valence Fock state, as it relates to the hadronic description in the constituent quark model. This state must have a very small size and hence a large mass. The higher terms are related to the sea components of the hadronic structure, and are larger and lighter. It has been shown that once the valence Fock state is determined, it is possible to build the rest of the light-cone wave function [2,3].

The essential part of the wave function is the hadronic distribution amplitude  $\phi(u, Q^2)$ . It describes the probability amplitude to find a quark and antiquark of the respective lowest-order Fock state carrying fractional momenta  $u$  and  $1 - u$ . For pions it is related to the light-cone wave function of the respective Fock state  $\psi$  through [4]

$$\phi_{q\bar{q}/\pi}(u, Q^2) \sim \int_0^{Q^2} \psi_{q\bar{q}/\pi}(u, \tilde{k}_{\perp}) d^2\tilde{k}_{\perp}, \quad (4)$$

$$Q^2 = \frac{k_{\perp}^2}{u(1-u)}. \quad (5)$$

The general form of the distribution amplitude is given by [4]

$$\phi_{\pi}(x, \mu^2) = x(1-x) \sum_{n \geq 0} a_n C_n^{3/2}(2x-1) \left(\ln \frac{\mu^2}{\Lambda^2}\right)^{-\gamma_n/2\beta_2}, \quad (6)$$

where  $C_n$  are the Gegenbauer polynomials,  $\gamma_n$  the anomalous dimensions. For many years, two functions were considered to describe the momentum distribution amplitude of the quark and antiquark in the  $|q\bar{q}\rangle$  configuration. The asymptotic function was calculated using perturbative QCD (pQCD) methods [4–6], and is the solution to the pQCD evolution equation for very large  $Q^2$  ( $Q^2 \rightarrow \infty$ )

$$\phi_{\text{Asy}}(u) = \sqrt{3}u(1-u) \quad (7)$$

corresponding to  $a_2 = 0$ ,  $a_4 = 0$ . Using QCD sum rules, Chernyak and Zhitnitsky (CZ) proposed [7] a function that is expected to be correct for low  $Q^2$

$$\phi_{\text{CZ}}(u) = 5\sqrt{3}u(1-u)(1-2u)^2 \quad (8)$$

corresponding to  $a_2 = 0.4$ ,  $a_4 = 0$ . Measurements of the electromagnetic form factors of the pion, traditionally used to study LCWF, are related to the integral over the wave function and the scattering matrix element, and their sensitivity to the shape of the wave function is low [8]. A differential measurement of the LCWF is therefore necessary.

The concept of the measurement presented here is the following: a high energy pion dissociates diffractively while interacting with a heavy nuclear target. The first (valence) Fock component dominates at large  $Q^2$ ; the other terms are suppressed by powers of  $1/Q^2$  for each additional parton, according to the counting rules [8,9]. This is a coherent process in which the quark and antiquark break apart and hadronize into two jets. If in this fragmentation process the quark momentum is transferred to the jet, measurement of the jet momentum gives the quark (and antiquark) momentum. Thus:  $u_{\text{measured}} = \frac{p_{\text{jet1}}}{p_{\text{jet1}} + p_{\text{jet2}}}$ . It has been shown by Frankfurt et al. [10] that the cross section for this process is proportional to  $\phi^2$ .

An important assumption is that quark momenta are not modified by nuclear interactions; i.e., that color transparency [6] is satisfied. The valence Fock state is far off-shell with mass  $M_n$  of several  $\text{GeV}/c^2$ . This corresponds to a transverse size of about 0.1 fm, much smaller than the regular pion size. Under these conditions, the valence quark configuration will penetrate the target nucleus freely and exhibit the phenomenon of color transparency. The lifetime of the configuration is given by  $2P_{\text{lab}}/(M_n^2 - M_\pi^2)$ , so at high beam momenta the configuration is kept small throughout its journey through the nucleus. Bertsch et al. [6] proposed that the small  $|q\bar{q}\rangle$  component will be filtered by the nucleus. Frankfurt et al. [10] show that for  $k_t > 1.5 \text{ GeV}/c$  the interaction with the nucleus is completely coherent and  $\sigma(|q\bar{q}\rangle N)$  is small. This leads to an  $A^2$  dependence of the forward amplitude squared. When integrated over transverse momentum, the signature for color transparency is a cross section dependence of  $A^{4/3}$ .

The basic assumption that the momentum carried by the dissociating  $q\bar{q}$  is transferred to the di-jets was examined by Monte Carlo (MC) simulations of the asymptotic and CZ wave functions (squared). The MC samples were allowed to hadronize through the LUND PYTHIA-JETSET model [11] and then passed through simulation of the experimental apparatus. While the fragmentation process and experimental effects smear somewhat the distributions, their qualitative features are retained.

## 1.2. Experimental results

Results of experimental studies of the pion light-cone wave function were recently published by the Fermilab E791 collaboration [12]. In the experiment, diffractive dissociation of 500  $\text{GeV}/c$  negative pions interacting with carbon and platinum targets was measured. Diffractive di-jets were required to carry the full beam momentum. They were identified through the  $e^{-bq_t^2}$  dependence of their yield ( $q_t^2$  is the square of the transverse momentum transferred to the nucleus and  $b = \langle R^2 \rangle / 3$  where  $R$  is the nuclear radius).

For the measurement of the wave function, the most forward events ( $q_t^2 < 0.015$  GeV/c<sup>2</sup>) from the platinum target were used. For these events, the value of  $u$  was computed from the measured longitudinal momenta of the jets. The analysis was carried out in two windows of  $k_t$ :  $1.25 \text{ GeV}/c \leq k_t \leq 1.5 \text{ GeV}/c$  and  $1.5 \text{ GeV}/c \leq k_t \leq 2.5 \text{ GeV}/c$ . The resulting  $u$  distributions are shown in Fig. 1. In order to get a measure of the correspondence between the experimental results and the calculated light-cone wave functions, the results were fit with a linear combination of squares of the two wave functions (after smearing).

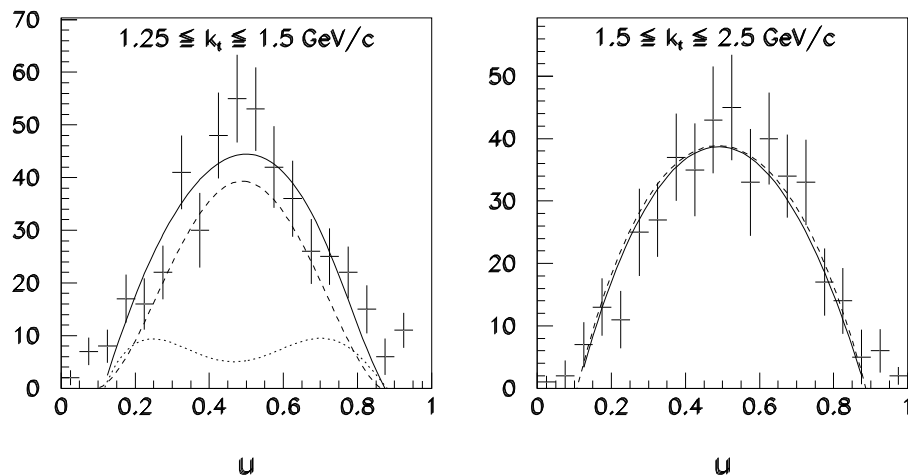


Fig. 1. The  $u$  distribution of diffractive di-jets from the platinum target for  $1.25 \leq k_t \leq 1.5 \text{ GeV}/c$  (left) and for  $1.5 \leq k_t \leq 2.5 \text{ GeV}/c$  (right). The solid line is a fit to a combination of the asymptotic and CZ wave functions. The dashed line shows the contribution from the asymptotic function and the dotted line that of the CZ function.

The results for the higher  $k_t$  window show that the asymptotic wave function describes the data very well. Hence, for  $k_t > 1.5 \text{ GeV}/c$ , which translates to  $Q^2 \sim 10 (\text{GeV}/c)^2$ , the pQCD approach that led to construction of the asymptotic wave function is reasonable. The distribution in the lower window is consistent with a significant contribution from the CZ wave function or may indicate contributions due to other non-perturbative effects. As the measurements are done within  $k_t$  windows, the results actually represent the square of the light-cone wave function averaged over  $k_t$  in the window:  $\psi_{\text{qq}}^2(x, \overline{k_\perp})$ .

The  $k_t$  dependence of diffractive di-jets is another observable that can show the region where perturbative calculations describe the data. As shown in Ref. [10], it is expected to be

$$\frac{d\sigma}{dk_t} \sim k_t^{-6}.$$

The results, shown in Fig. 2, are consistent with this dependence only in the region

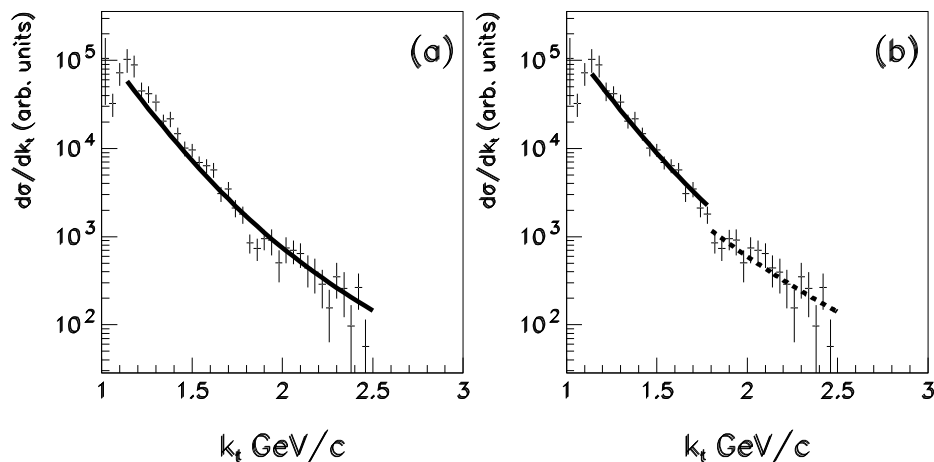


Fig. 2. Comparison of the  $k_t$  distribution of acceptance corrected data with fits to cross section derived from (a) two-terms singlet-model wave function [13]. (b) Two-term wave function for low  $k_t$ , and a power law, as expected from perturbative calculations, for high  $k_t$ .

above  $k_t \sim 1.8$  GeV/c, in agreement with the conclusions from the  $u$ -distributions. For lower  $k_t$  ( $Q^2$ ) values, non-perturbative effects are expected to be significant [13].

Finally, verification that the  $|q\bar{q}\rangle$  configuration is small and does not suffer from final state nuclear interaction was done by observing the color transparency effect for the diffractive di-jets. The  $A$ -dependence of the diffractive di-jet yield was measured and found to have  $\sigma \propto A^\alpha$  with  $\alpha \sim 1.5$ , consistent with the expected color transparency signal [10].

## 2. The photon light-cone wave function

### 2.1. Theoretical considerations

The photon light-cone wave function can be described in a similar way except that it has two major components: the electromagnetic and the hadronic states

$$\begin{aligned} \psi_\gamma = & a|\gamma_p\rangle + b|l^+l^-\rangle + c|l^+l^-\gamma\rangle + (\text{other e.m.}) \\ & + d|q\bar{q}\rangle + e|q\bar{q}g\rangle + (\text{other hadronic}) + \dots, \end{aligned} \quad (9)$$

where  $|\gamma_p\rangle$  describes the point bare-photon and  $|l^+l^-\rangle$  stands for  $|e^+e^-\rangle$ ,  $|\mu^+\mu^-\rangle$  etc. Each of these states is a sum over the relevant helicity components. The wave function is very rich: it can be studied for real photons, for virtual photons of various virtualities, for transverse and longitudinal photons, and the hadronic component

may be decomposed according to the quark's flavor. The LCWF for the lowest Fock states is given by [14]

$$\psi_{\lambda_1\lambda_2}^\lambda(k_\perp, u) = -ee_f \frac{\bar{f}_{\lambda_1}(k)\lambda \cdot \epsilon^\lambda f_{\lambda_2}(q-k)}{\sqrt{u(1-u)} \left( Q^2 + \frac{k_\perp^2 + m^2}{u(1-u)} \right)}, \quad (10)$$

where  $\epsilon^\lambda$  is the polarization vector and  $f_\lambda$ ,  $m$ ,  $\lambda_1$ ,  $\lambda_2$ ,  $ee_f$  are the fermion distributions, masses, helicities and charges, respectively.  $Q^2$  is the photon virtuality. The wave function for  $k_\perp^2 \gg \Lambda_{\text{QCD}}^2$  is expected to be similar for the electromagnetic and hadronic components. The probability amplitude  $\Phi^2$  is obtained from the trace of this function. For transversely polarized photon the result is:

$$\Phi_{\text{ff}/\gamma_T^*}^2 \sim \sum_{\mu=1}^2 \frac{1}{4} \text{Tr} \psi^2 = \frac{m^2 + k_\perp^2 [u^2 + (1-u)^2]}{[k_\perp^2 + a^2]^2}, \quad (11)$$

where  $a^2 = m^2 + Q^2 u(1-u)$ . The predicted LCWF for the electromagnetic component are based on quantum electrodynamics and can be considered precise. Those for the hadronic component are model dependent. Examples of  $\Phi^2$  calculated using Eq. (3) and the asymptotic LCWF suggested for the hadronic component [15] are shown in Fig. 3.

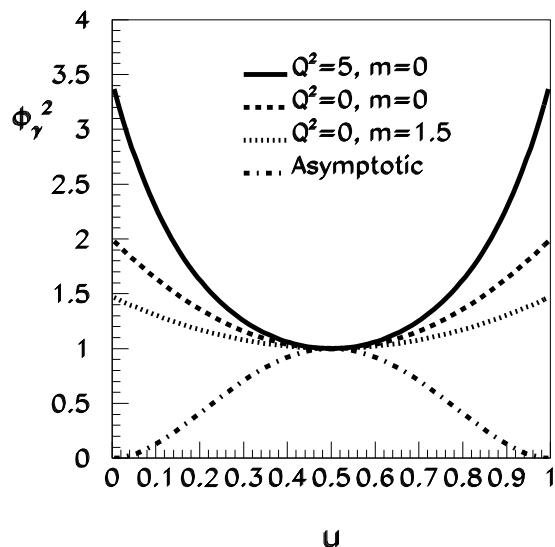


Fig. 3. The photon wave function for transverse virtual photons ( $Q^2 = 5 \text{ (GeV/c)}^2$ ) and massless quarks/leptons (solid line), real photons and massless quarks/leptons (dashed line), real photons and charm quarks (dotted line) and the asymptotic function (dashed-dotted line). The functions are arbitrarily normalized at  $u = 0.5$ .

## 2.2. Measurement of the electromagnetic component of real photon LCWF

Measurement of the photon light-cone wave function is being carried out at the DESY accelerator in the collision of 28 GeV/c electrons (or positrons) with 920 GeV/c protons producing real or virtual photons. The measurements were done using the ZEUS detector [16]. Measurement of the electromagnetic component of the real photon LCWF was done using the exclusive  $ep \rightarrow e\mu^+\mu^-p$  photoproduction process.

### 2.2.1. Data analysis

The integrated luminosity for the results presented here was  $55.4 \pm 1.3 \text{ pb}^{-1}$ . Events of the exclusive reaction were triggered using the muon chambers. Each event was required to have two high quality tracks fitted to the vertex and matched to energy deposits in the calorimeter. It was required that no signal from the scattered positron or from proton dissociation be recorded. The LCWF was measured as the distribution of the longitudinal light-cone momentum fraction as defined in Eq. (2) (see Fig. 4)

$$u = \frac{E_1 + p_{z1}}{E_1 + p_{z1} + E_2 + p_{z2}}, \quad (12)$$

where  $E_1, p_1, E_2, p_2$  are the energy and momentum of each muon. The kinematic region was defined by the following selection criteria: the invariant mass of the dimuon system  $4 \text{ GeV} < M_{\mu\mu} < 15 \text{ GeV}$ , the  $\gamma p$  centre of mass energy  $30 \text{ GeV} < W < 170 \text{ GeV}$  (in order to remain in a region of stable and high acceptance), the square of the four momentum exchanged at the proton vertex  $|t| < 0.5 \text{ GeV}^2$  (to select diffractive events),  $0.1 < u < 0.9$  (to avoid region of low acceptance) and  $k_T > 1.2 \text{ GeV}$  (to select a hard process). The acceptance corrections and resolutions were determined using dedicated Monte Carlo GRAPE generator [17] for dilepton

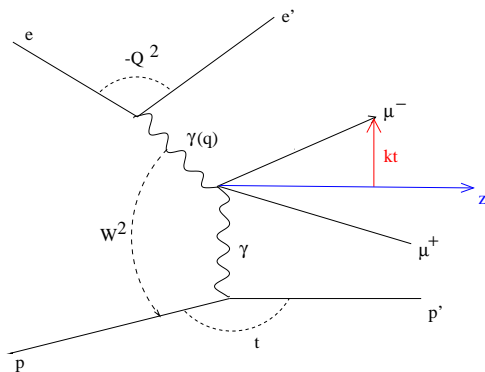


Fig. 4. Definition of the kinematic variables.

production in ep collisions, based on exact matrix elements. The program is interfaced to PYTHIA to generate a complete final state. The simulation included both elastic and proton-dissociative events. All generated events were passed through a detector simulation based on GEANT 3.13.

### 2.2.2. Results and discussion

The measured  $k_T$ ,  $W$ ,  $t$ ,  $M_{\mu\mu}$  distributions are presented in Fig. 5. The data are compared with GRAPE Monte Carlo simulation normalized to the data. Good agreement is shown between data and simulation. The measured differential cross section  $d\sigma/du$  is presented in Fig. 6 and compared with the theoretical curve (BFGMS) [14]. For this purpose, Eq. (11) was adapted to the muon's analysis

$$\Phi_{\mu\mu/\gamma}^2 = \frac{u^2 + (1-u)^2}{M_{\mu\mu}^2 u(1-u) - m_\mu^2}. \quad (13)$$

## ZEUS

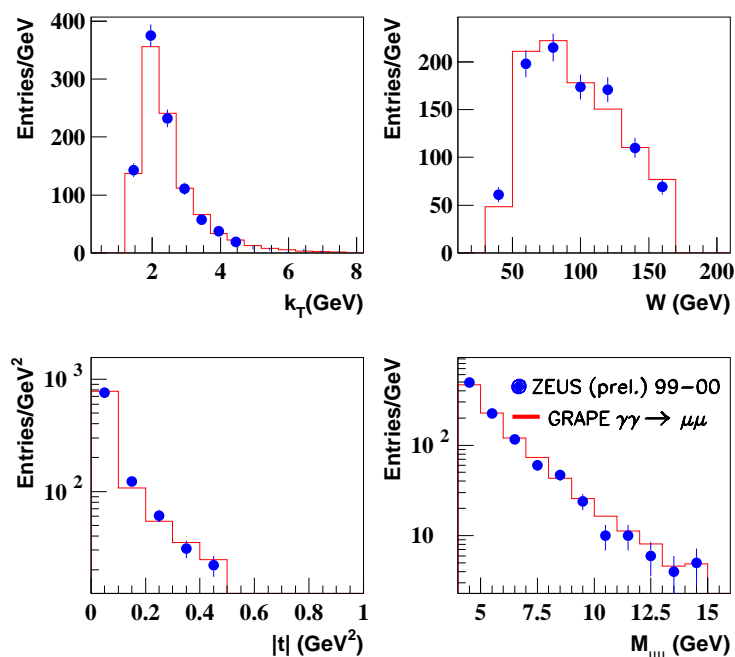


Fig. 5. Number of events reconstructed in the kinematic region  $4 \text{ GeV} < M_{\mu\mu} < 15 \text{ GeV}$ ,  $30 \text{ GeV} < W < 170 \text{ GeV}$ ,  $|t| < 0.5 \text{ (GeV/c)}^2$  and  $k_T > 1.2 \text{ GeV/c}$  plotted against  $k_T$ ,  $W$ ,  $|t|$  and  $M_{\mu\mu}$ . The data distributions are shown as the points with statistical errors only. The solid lines show the prediction of the GRAPE generator summing elastic and proton-diffractive components.



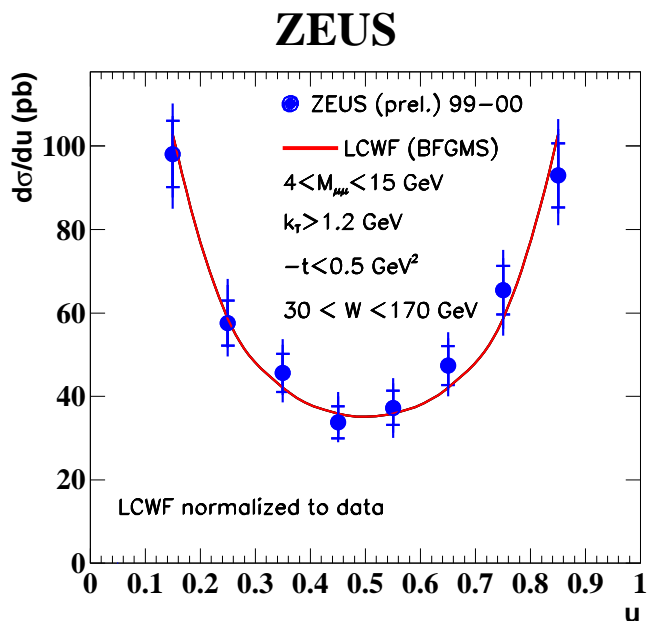


Fig. 6. Differential cross section  $d\sigma/du$  measured for  $30 \text{ GeV} < W < 170 \text{ GeV}$ ,  $4 \text{ GeV} < M_{\mu\mu} < 15 \text{ GeV}$ ,  $k_T > 1.2 \text{ GeV}/c$  and  $-t < 0.5 (\text{GeV}/c)^2$ . The inner error bars show the statistical uncertainty; the outer error bars show the statistical and systematics added in quadrature. The data points are compared to the prediction of LCWF theory [14]. The theory is normalized to data.

The LCWF was normalized to the data. The shape of calculated electromagnetic component of the real photon light-cone wave function is in good agreement with the experimental result. The measured cross section was also compared to the GRAPE simulation normalized to the luminosity. The agreement between data and simulation is within the systematic uncertainties.

This measurement serves as “Standard Candle” and normalization for the Hadronic LCWF. It also provides the first proof that diffractive dissociation of particles can be reliably used to measure their LCWF. Furthermore it gives support for the method used in previous measurements of the pion LCWF [12] and possible future applications to other hadrons [18].

#### *Acknowledgements*

I would like to thank Drs. S. Brodsky and L. Frankfurt for many helpful discussions. I also want to acknowledge the efforts of the E791 and ZEUS collaborations for the data presented in this work.

This work is supported in part by the Israel Science Foundation and the US-Israel Binational Science Foundation.

References

- [1] S. J. Brodsky, D. S. Hwang, B. Q. Ma and I. Schmidt, Nucl. Phys. B **593** (2001) 311.
- [2] A. H. Mueller, Nucl. Phys. B **415** (1994) 373; F. Antonuccio, S. J. Brodsky and S. Dalley, Phys. Lett. B **412** (1997) 104.
- [3] S. Daley, *Proc. 10th Light Cone Meeting*, Heidelberg, 2000, hep-ph/0007081.
- [4] S. J. Brodsky and G. P. Lepage, Phys. Rev. D **22** (1980) 2157; S. J. Brodsky and G. P. Lepage, Phys. Scripta **23** (1981) 945; S. J. Brodsky, *Springer Tracts in Modern Physics* **100** (1982) 81.
- [5] A. V. Efremov and A. V. Radyushkin, Theor. Math. Phys. **42** (1980) 97.
- [6] G. Bertsch, S. J. Brodsky, A. S. Goldhaber and J. Gunion, Phys. Rev. Lett. **47** (1981) 297.
- [7] V. L. Chernyak and A. R. Zhitnitsky, Phys. Rep. **112** (1984) 173.
- [8] G. Sterman and P. Stoler, Ann. Rev. Nuc. Part. Sci. **43** (1997) 193.
- [9] S. J. Brodsky and G. R. Farrar, Phys. Rev. Lett. **31** (1973) 1153.
- [10] L. L. Frankfurt, G. A. Miller and M. Strikman, Phys. Lett. B **304** (1993) 1.
- [11] H.-U. Bengtsson and T. Sjöstrand, Comp. Phys. Comm. **82** (1994) 74; T. Sjöstrand, PYTHIA 5.7 and JETSET 7.4 Physics and Manual, CERN-TH.7112/93, (1995).
- [12] E. M. Aitala et al., E791 Collaboration, Phys. Rev. Lett. **86** (2001) 4768; **86** (2001) 4773.
- [13] D. Ashery and H. C. Pauli, Eur. Phys. J. C **28** (2003) 329.
- [14] S. J. Brodsky, L. Frankfurt, J. F. Gunion, A. H. Mueller and M. Strikman, Phys. Rev. D **50** (1994) 3134.
- [15] I. I. Balitsky et al., Nucl. Phys. B **312** (1989) 509.
- [16] U. Holm et al., ZEUS Collaboration, The ZEUS Detector (unpublished), DESY (1993), [www-zeus.desy.de/bluebook/bluebook.html](http://www-zeus.desy.de/bluebook/bluebook.html).
- [17] T. Abe et al., *Proc. Workshop on Monte Carlo Generators for HERA Physics*, eds. T.A. Doyle et al., DESY (1999).
- [18] D. Ashery, Comments on Modern Physics **2A** (2002) 235.

MJERENJE VALNIH FUNKCIJA NA SVJETLOSNOJ KONUSI  
DIFRAKTIVNOM DISOCIJACIJOM

Valne funkcije čestica na svjetlosnoj konusi mogu se proučavati njihovom difrakcijskom disocijacijom. Predstavljamo ishode mjerenja E791 u Fermilabu i mjerenja HERA/ZEUS u DESYju.